Nanoscale

PAPER

View Article Online
View Journal

Cite this: DOI: 10.1039/c5nr04881h

Insulin-coated gold nanoparticles as a new concept for personalized and adjustable glucose regulation

Malka Shilo,[a] Peter Berenstein,[b] Tamar Dreifuss,[a] Yuval Nash,[c,d] Guy Goldsmith,[c] Gila Kazimirsky,[b] Menachem Motiei,[a] Dan Frenkel,[c,d] Chaya Brodie[b] and Rachela Popovtzer*[a]

Received 21st July 2015,
Accepted 15th October 2015

DOI: 10.1039/c5nr04881h

www.rsc.org/nanoscale

Diabetes mellitus is a chronic metabolic disease, characterized by high blood glucose levels, affecting millions of people around the world. Currently, the main treatment for diabetes requires multiple daily injections of insulin and self-monitoring of blood glucose levels, which markedly affect patients' quality of life. In this study we present a novel strategy for controlled and prolonged glucose regulation, based on the administration of insulin-coated gold nanoparticles (INS-GNPs). We show that both intravenous and subcutaneous injection of INS-GNPs into a mouse model of type 1 diabetes decreases blood glucose levels for periods over 3 times longer than free insulin. We further showed that conjugation of insulin to GNPs prevented its rapid degradation by the insulin-degrading-enzyme, and thus allows controlled and adjustable bio-activity. Moreover, we assessed different sizes and concentrations of INS-GNPs, and found that both parameters have a critical effect *in vivo*, enabling specific adjustment of blood glucose levels. These findings have the potential to improve patient compliance in diabetes mellitus.

Introduction

Type 1 and type 2 diabetes mellitus are chronic, lifelong diseases characterized by high blood glucose levels (hyperglycemia). Chronic hyperglycemia may cause several serious diseases such as kidney failure, heart disease, ketoacidosis, stroke, and blindness. The main treatment today is based on subcutaneous injection of external insulin to decrease glucose levels to the normal range (80–120 mg dl^{-1}).[1,2] In type 1 diabetes these injections contain a mixture of short and long-acting insulin to deal with both basal requirements and the boost which is needed after meals. However, this treatment requires multiple daily injections of insulin and self-monitoring of blood glucose levels, which in addition to the disease itself, markedly affect patients' quality of life.[3–5]

Over the last decade, nanoparticles have gained attention as promising drug delivery agents. Several studies demonstrated that the use of different types of nanoparticles,[6–10] and specifically gold nanoparticles[11–14] for insulin delivery mainly through transmucosal,[6,11,12] oral[7,8] or transdermal[9,10,13,14] routes, increased serum insulin levels and improved the glycemic response to glucose challenge for an extended period of time.[8] However, despite the major advantage of non-invasive administration routes, several drawbacks exist. By following transmucosal and oral administration, nanoparticle bioavailability in blood is low due to poor transport across the intestinal epithelium, and drug activity is challenged by gastrointestinal acids and enzymes.[7,8,12] For transdermal administration, the lag time for a drug to penetrate through the skin to the systemic circulation is a major limiting factor, therefore this procedure is unsuitable for drugs that require rapid onset of action. Moreover, drugs required at high levels in blood cannot be administered transdermally.[15,16] Therefore, new treatment strategies are needed, which provide timely, prolonged, and efficient regulation of blood glucose.

In the present study, we examine a novel strategy for glucose regulation, based on intravenous administration of insulin-coated gold nanoparticles (INS-GNPs). We chose GNPs as a model system due to their various advantages, including a high degree of flexibility in terms of particle size and shape, the array of possible functional groups for coating and targeting, their long circulation time, and biosafety.[17–21] The potential for clinical implementation of GNPs has led to substantial research on their *in vivo* chemical stability,[22–24] pharmacokinetics,[22] biodistribution[24–29] and bio-toxicity.[22,25,30–33]

[a]*Faculty of Engineering & Institutes of Nanotechnology & Advanced Materials, Bar-Ilan University, Ramat-Gan, 5290002, Israel. E-mail: rachela.popovtzer@biu.ac.il*
[b]*Everard and Mina Goodman Faculty of Life Sciences, Bar-Ilan University, Ramat-Gan, 5290002, Israel*
[c]*Department of Neurobiology & Sagol School for Neuroscience, George S. Wise Faculty of Life Sciences, Tel Aviv University, Tel Aviv, 6997801 Israel*
[d]*Department of Neurobiology, George S. Wise Faculty of Life Sciences, Tel Aviv University, Tel Aviv, 6997801 Israel*

In this study we show the adjustable and controlled systemic effect of INS-GNPs on glucose regulation, which potentially can be used for personalized diabetic treatment. INS-GNPs were physicochemically characterized (diameter, zeta-potential and insulin loading), and their resistance to enzymatic degradation was examined *in vitro*. The effect of different sizes and concentrations of INS-GNPs on blood glucose levels was tested in Balb/c mice. In addition, the effect of INS-GNPs on blood glucose levels in comparison with free insulin was tested in diabetic mice.

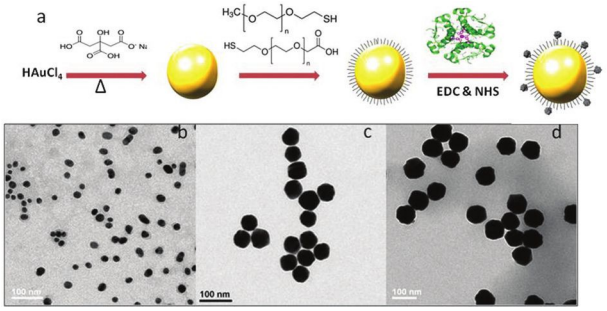

Fig. 1 Synthesis and characterization of INS-GNPS: (a) schematic diagram of the synthesis of 20 nm GNPs and functionalization with insulin. (b–d) TEM images of 20, 50 and 70 nm GNPs, respectively (scale bar 100 nm).

Experimental

Synthesis of 20 nm GNPs

GNPs were synthesized by citrate reduction of hydrogen tetrachloroaurate(III) trihydrate ($HAuCl_4$, Strem).[34] 414 μL of 50% w/v $HAuCl_4$ solution in 200 mL purified water was boiled in an oil bath on a heating plate while being stirred. After boiling, 4.04 mL of 10% trisodium citrate solution was added and the mixture was stirred while boiling for another 10 minutes. The solution was centrifuged until precipitation of nanoparticles and a clear suspension was obtained.

Synthesis of seed solution for GNPs at 50 and 70 nm

10 mL of purified water was mixed with 10.4 μL of 50% w/v $HAuCl_4$ solution. The solution was stirred and boiled on a heating plate. To the stirred solution, 100 μL of Na_3 citrate (8.8 wt%) was added and the mixture was stirred and boiled for another 5 minutes. Then, the solution was diluted with water to a volume of 50 mL, which can be used for an hour after the preparation.

Synthesis of 50 and 70 nm GNPs in growth solution

For both sizes, 200 mL of purified water was mixed with 6.5 mL seed solution. 88 μL of 50% w/v $HAuCl_4$ and 7.5 mL of 0.04 M MSA solution were added while stirring and 176.8 μL of 50% w/v $HAuCl_4$ solution and 15 mL of 0.04 M MSA solution were added while stirring for the synthesis of 50 and 70 nm GNPs, respectively. The mixtures were stirred for another half an hour.

Conjugation of PEG layer and insulin to the GNPs

GNPs were coated with a layer of PEG (Creative PEGWorks, Winston Salem, NC, USA) composed of a mixture of mPEG-SH (85%) and SH-PEG-COOH (15%). This mixture was then stirred for three hours. The PEG layer was covalently conjugated to human insulin (1.5 ml, 100 IU ml^{-1}, Novo Nordisk A/S, Denmark) by adding excess 1-ethyl-3-(3-dimethylaminopropyl) carbodiimide HCl (EDC, 200 μl, Thermo Scientific, USA) and *N*-hydroxysulfosuccinimide sodium salt (NHS, 200 μl, Thermo Scientific, USA) (Fig. 1a). The mixture was subsequently stirred overnight, and the INS-GNPs were purified after the solution was centrifuged, until a clear suspension was obtained. The final concentration of the INS-GNPs was 30 mg ml^{-1}.

GNP characterization

The size, shape and uniformity of the GNPs were measured using a transmission electron microscope (TEM) (JEM-1400, JEOL). The samples were prepared by drop-casting 5 μL of the GNP solution onto a standard carbon-coated film on a copper grid. The samples were left to dry in a vacuum desiccator. The GNPs were further characterized using a ultraviolet-visible spectrophotometer (UV-1650 PC; Shimadzu Corporation, Kyoto, Japan) at each level of coating. Conjugation of insulin to the GNPs was verified using zeta-potential measurements (ZetaSizer 3000HS; Malvern Instruments, Malvern, UK).

Human insulin ELISA

The amount of insulin that was conjugated to GNPs was determined by using a human insulin ELISA kit, performed as described by the manufacturer (Moshe Stauber Biotech Applications, Mercodia), based on the direct "sandwich" technique, in which two monoclonal antibodies are directed against separate antigenic determinants on the insulin molecule. Due to the 3D structure of the GNPs, the excess of insulin in serum after the synthesis of INS-GNPs was tested according to the following formula:

$$100 \times \frac{\text{Total amount of insulin added} - \text{Amount of excess insulin in serum}}{\text{Total amount of insulin added}} \quad (1)$$

Insulin degradation by IDE

96-well ELISA plates (Nunc, Denmark) were coated overnight at 4 °C with 5 μg ml^{-1} recombinant insulin degrading enzyme (IDE) diluted in a buffer containing 100 mM Tris-HCl (pH 7.5), 50 mM NaCl and 10 μM $ZnSO_4$. Additional wells were not

coated with IDE, and served as control. All the wells were washed 3 times with PBS with 0.05% Tween (PBST), and blocked overnight at 4 °C with 3% skim milk in PBS. Wells were loaded with different concentrations of insulin and were shaken for 2 hours at 120 rpm at 37 °C. 10 μL of the supernatant were taken and measured for the remaining insulin content using a Mercodia Mouse Insulin ELISA kit (cat #10-1247-01, Mercodia, Sweden), according to the manufacturer's protocol. Data were analyzed using two-way ANOVA followed by *post hoc* analysis with Bonferroni, using STATISTICA v.12 (StatSoft, Tulsa, OK, USA).

Animals

To examine the effect of the INS-GNP size on blood glucose levels, male Balb/c mice weighing 20–25 g were used. To test 50 nm INS-GNPs in the diabetic model, male non-obese diabetic (NOD) mice weighing 20–25 g were used. Mice were considered to be diabetic when their blood glucose levels were above 200 mg dl^{-1} (as measured by using a glucometer (FreeStyle Lite, Abbott)). All mice were subjected to fasting during the experiments. The study was approved by the Animal Care and Use Committees of Bar Ilan University, Ramat Gan, Israel.

Effect of GNP size

Balb/c mice were divided into three groups (n = 3 for each group), injected with either 20 nm, 50 nm or 70 nm INS-GNPs (30 mg ml^{-1}, 200 μl for all sizes) into the tail vein. Blood glucose levels of the mice were monitored every hour, up to 6 h post-injection, using a glucometer (FreeStyle Lite, Abbott) on a blood sample from the mice tail. Relative activity after this experiment, and all subsequent experiments, was calculated by dividing the blood glucose levels at each timepoint by baseline levels measured before treatment administration (considered as 100%), according to the formula:

$$100 \times \frac{\text{Measured blood glucose level}}{\text{Baseline blood glucose level}}. \quad (2)$$

Effect of GNP concentration

Balb/c mice were divided into three groups (n = 3 for each group), injected with either 1.875 mg ml^{-1}, 7.5 mg ml^{-1} or 30 mg ml^{-1} of 50 nm INS-GNPs (200 μl for all concentrations) into the tail vein. Blood glucose levels of mice were monitored every hour, up to 6 h post-injection, using a glucometer (FreeStyle Lite, Abbott) on a blood sample from the mice tail.

Pharmacokinetics of INS-GNPs within the blood

Balb/c mice were divided into three groups (n = 3 for each group), injected with either 20 nm, 50 nm or 70 nm INS-GNPs (30 mg ml^{-1}, 200 μl for all sizes) into the tail vein. The mice were anesthetized and blood samples were taken for analysis every hour up to six hours post-injection by Flame Atomic Absorption Spectroscopy (FAAS).

Pharmacokinetics and biodistribution of INS-GNPs

Balb/c mice were divided into three groups (n = 3 for each group), injected with either 20 nm, 50 nm or 70 nm INS-GNPs (30 mg ml^{-1}, 200 μl for all sizes) into the tail vein. The mice were anesthetized and sacrificed at 0.5, 2, 24 and 48 hours post-injection and their main organs (including liver, pancreas, spleen, kidney and blood samples) were taken for analysis by FAAS.

Effect of INS-GNPs on diabetic mice

NOD mice were divided into two groups (n = 3 for each group). The treatment group received an injection of 30 mg ml^{-1} of 50 nm INS-GNPs (200 μl) into the tail vein. The control group received an IV injection (into the tail vein) of 0.12 IU insulin (human insulin, 100 IU ml^{-1}, Novo Nordisk A/S, Denmark), which was the same amount of insulin found be bound to the 50 nm INS-GNPs, in the initial ELISA test. Blood glucose levels of mice were monitored every 0.5 h, up to 6.5 hours post-injection, using a glucometer on a blood sample from the mice tail.

Glucose tolerance test

NOD mice were divided into two groups of three mice each, which received an injection of either 30 mg ml^{-1} of 50 nm INS-GNPs (200 μl), or 0.12 IU of free insulin as control, into the tail vein. Two hours post-injection, α-D-glucose was injected into the tail vein based on the initial blood glucose values. Blood glucose levels of mice were monitored by using a glucometer every half an hour, up to 5 h post-initial treatment injection.

Subcutaneous injection

NOD mice were divided into two groups, which received a subcutaneous injection of either 30 mg ml^{-1} of 50 nm INS-GNPs (200 μl) (n = 3) or 0.12 IU of free insulin as control (n = 2). Blood glucose levels of the mice were monitored using a glucometer every 0.5 hour, up to 5 h post-injection.

Determination of the amount of GNPs in mice organs

Flame Atomic Absorption Spectroscopy (FAAS, SpectrAA 140, Agilent Technologies) was used to determine the amount of gold in the investigated samples. The samples were melted with aqua regia acid (a mixture of nitric acid and hydrochloric acid in a volume ratio of (1 : 3)), filtered and diluted to a final volume of 10 ml. The calibration curve with known gold concentrations was prepared and the gold concentration was determined according to absorbance values, compared to calibration curves. All samples were analyzed by FAAS under the same experimental conditions.

Statistical analysis

Data were presented as mean ± S.D. Statistical analysis was performed using the Mann–Whitney U-test and the significance of $p < 0.05$ was considered significant. In insulin degradation by IDE test, *post-hoc* test was performed and the significance of $p < 0.05$ was considered significant.

Results and discussion

GNP-synthesis and conjugation

Particle size, shape, and uniformity were measured using TEM, showing that spherical, uniformly distributed GNPs were obtained, in diameters of 20, 50 and 70 nm (Fig. 1b–d). INS-GNPs were characterized after each preparation step, using ultraviolet-visible spectroscopy. An expanded signal was observed after each layer of coating, confirming the chemical coating (Fig. 2). Changes in zeta-potential values further confirmed the chemical coating (Fig. 2).

In vitro assays

Quantification of insulin bound to GNPs. The number of insulin molecules that bind to each 20 nm GNP was quantified using a human insulin ELISA assay. We found that each nanoparticle was coated with 50 molecules of insulin, which is in accord with theoretical calculations.[35] Thus, for the subsequent *in vivo* experiments below, we determined that the mice treated with 200 μl of 30 mg ml^{-1} of 50 nm INS-GNPs (7.42×10^{13} nanoparticles) received an amount of bound insulin that is equivalent to 0.12 IU of free insulin (6 IU kg^{-1}).

In vivo experiments

The effect of differently sized INS-GNPs on glucose regulation. The size of NPs has a crucial effect on blood circulation half-life, and therefore bioactivity, after intravenous injection.[36] Therefore, we examined the effect of the INS-GNP size on bioactivity by measuring blood glucose levels in mice over time. INS-GNPs of different diameters – 20, 50 and 70 nm, were injected into the tail vein of Balb/c mice. Blood glucose levels were measured before injection, and every hour post-injection, up to 6 h. As demonstrated in Fig. 3, we found that for all GNP sizes, the blood glucose levels decreased immediately after injection, and reached their lowest value 2 h post-injection. The blood glucose levels began to raise 2 h post-injection for 20 nm INS-GNPs, and only 4 h post-injection for 50 and 70 nm INS-GNPs. The 50 nm INS-GNPs significantly decreased the blood glucose levels up to 6 h, as compared to the other sizes (according to the Mann–Whitney *U* test $p < 0.05$). Therefore, the 50 nm INS-GNPs were chosen as the ideal sized particles for the subsequent experiments in diabetic mice. Our results show that by changing the size and concentration of the INS-GNPs, the extent of insulin activity can also be modulated and controlled, in accordance with the personal need. In order to verify that the optimal INS-GNP concentration is being utilized, the effect of different concentrations of INS-GNPs was examined. 50 nm INS-GNPs at different concentrations, 30, 7.5 and 1.875 mg ml^{-1} (equals to insulin dose of 1.12 IU, 0.28 IU and 0.07 IU, respectively), were injected into the tail vein of Balb/c mice. Blood glucose levels were measured before the injection and then every hour, up to 6 h post-injection. As demonstrated in Fig. 4, the blood glucose levels decreased immediately after injection for all INS-GNP concentrations.

One hour post-injection of either 1.875 mg ml^{-1} or 7.5 mg ml^{-1} INS-GNPs, the blood glucose levels reached a minimum of 57% and 29% of the baseline value, respectively, and then began to increase. For 30 mg ml^{-1} INS-GNPs, the blood glucose levels decreased to 10% of baseline one hour post-INS-GNP injection, up to at least four hours, and started to increase only five hours post-injection. Thus, this concentration was chosen for subsequent experiments. These results show that different parameters of INS-GNPs have a critical effect on insulin bioactivity. Controlling the concentration and size of INS-GNPs can extend the duration of insulin activity. These findings could promote personalized treatments that enable individual adjustment of the blood glucose levels in diabetic patients.

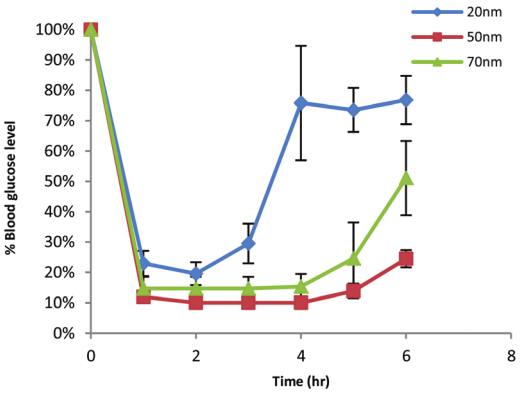

Fig. 3 Effect of INS-GNP size on blood glucose levels: 30 mg ml^{-1} INS-GNPs of different sizes (20, 50 and 70 nm) were injected into the tail vein of Balb/c mice. Blood glucose levels were monitored every hour, up to 6 h post-injection. The results are presented as percentage of blood glucose levels, mean ± S.D. *$p < 0.05$ 50 nm *vs.* 20 nm INS-GNPs. *U*-Test value = 0.0385.

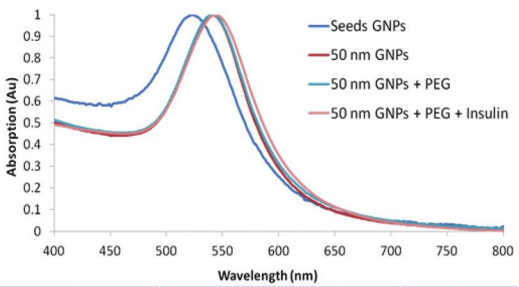

	20 nm	50 nm	70 nm
GNPs	-38±2	-40±0.4	-34±1
GNPs + PEG	-21±0.4	-44±0.6	-40 ±0.6
GNPs + PEG + Insulin	-27±0.6	-44±0.3	-48±0.3

Fig. 2 Characterization of the chemical coating: top: ultraviolet-visible spectroscopy of the bare GNPs, PEG coated GNPs, and INS-GNPs, for the 50 nm sized particles. Bottom: zeta-potential measurements at the various stages of GNP coatings, for each GNP size. A significant difference was obtained in zeta potential following each chemical step, demonstrating the efficiency of the chemical coating.

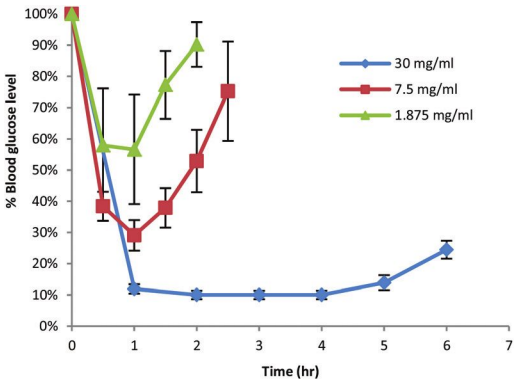

Fig. 4 Effect of INS-GNP concentrations on blood glucose levels: INS-GNPs at different concentrations (30, 7.5 and 1.875 mg ml^{-1}) were injected into the tail vein of Balb/c mice. Blood glucose levels were monitored every hour, up to 6 h post-injection. The results are presented as percentage of blood glucose levels, mean ± S.D.

(a)	0.5 h	2 h	24 h	48 h
Liver + Pancreas	0.18 ± 0.06	0.1 9± 0.03	0.34 ± 0.08	0.18 ± 0.05
Spleen	0.18 ± 0.06	0.31 ± 0.08	0.05 ± 0.03	0.18 ± 0.09
Kidney	0.2 ± 0.1	0.32 ± 0.03	0.17 ± 0.06	0.25 ± 0.05
Blood	0.04 ± 0.02	0.29 ± 0.13	0.14 ± 0.08	0.18 ± 0.09

(b)	0.5 h	2 h	24 h	48 h
Liver + Pancreas	0.28 ± 0.05	0.24 ± 0.13	0.23 ± 0.1	0.25 ± 0.22
Spleen	0.29 ± 0.12	0.25 ± 0.005	0.68 ± 0.46	0.52 ± 0.03
Kidney	0.22 ± 0.12	0.24 ± 0.07	0.08 ± 0.03	0.06 ± 0.01
Blood	0.28 ± 0.18	0.08 ± 0.002	0.004 ± 0.003	0.002 ± 0.001

(c)	0.5 h	2 h	24 h	48 h
Liver + Pancreas	0.12 ± 0.02	0.14 ± 0.01	0.3 ± 0.04	0.17 ± 0.17
Spleen	0.23 ± 0.07	0.24 ± 0.06	7.44 ± 7.07	0.37 ± 0.14
Kidney	0.006 ± 0.007	0.07 ± 0.04	0.19 ± 0.07	0.07 ± 0.01
Blood	0.24 ± 0.12	0.01 ± 0.007	0.008 ± 0.004	0.004 ± 0.002

Fig. 6 Pharmacokinetics and biodistribution of INS-GNPs (a) 20 nm, (b) 50 nm and (c) 70 nm. The results are presented as mg gold per g tissue.

In order to examine the relationship between blood circulation time of each particle size and lowering of blood glucose levels, we compared the amount of gold in blood for the different particle sizes, up to six hours post-injection (Fig. 5). We found that the amount of gold in blood for 20 nm particles was significantly higher than that of the 50 and 70 nm particles, at all timepoints examined. As the amount of gold indicates the amount of particles and the concentration of bound insulin for each particle size, we would expect the 20 nm particles to have an optimal effect on blood glucose levels and the longest activity duration. However, our results (Fig. 3) reveal that the 50 nm particles were the most effective. Therefore, we assume that the effect of INS-GNPs on blood glucose levels is complex and depends on various factors, making it difficult to isolate only one variable. The present study examined two important factors, *i.e.*, the size and concentration of the particles, serving as a foundation for future studies to determine other possible factors that impact the blood glucose levels.

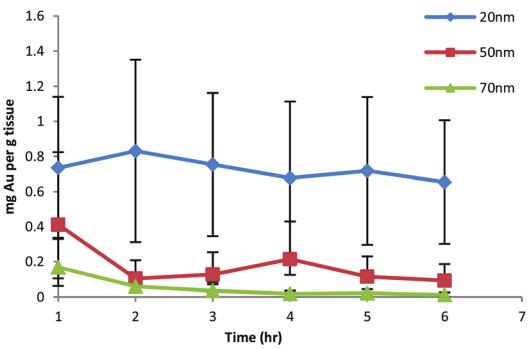

Fig. 5 Pharmacokinetics of INS-GNPs within the blood: gold amount measurements of 20, 50 and 70 nm INS-GNPs that were injected IV up to 6 hours post-injection, mean ± S.D.

We also performed an additional experiment to examine the pharmacokinetics and biodistribution of the different particle sizes, by measuring the concentration of the particles in blood and their accumulation in liver and pancreas, at several timepoints over a period of 48 hours (Fig. 6). We found that for 20 and 70 nm, the particles accumulate in liver and pancreas over time with a peak at 24 h, and for 50 nm the accumulation is somewhat constant. However, this accumulation is not significantly higher at timepoints for which blood glucose levels are low, as compared to other timepoints. In addition, each particle size had different pharmacokinetics and biodistribution. These results indicate that the particle circulation time is not a determining factor for long-term insulin activity. Future studies should determine various factors, such as variation in effective insulin loading, differences in biodistribution into cells/organs, variation in release/delivery of glucose or size-dependent variation in the insulin degradation rate, that affect the extent of insulin activity.

Bioactivity of intravenously injected INS-GNPs in type 1 diabetic mice. Next, we tested the effect of INS-GNPs on blood glucose levels in an animal model for type 1 diabetes. 50 nm INS-GNPs (30 mg ml^{-1}, 200 μl), or free insulin (0.21 IU) as control, were injected (IV) into NOD mice. We found that the blood glucose levels decreased immediately after the injection of either INS-GNPs or free insulin (Fig. 7). However, for INS-GNPs, the blood glucose levels remained low even 6 h post-injection, and reached only 70% of baseline after 6.5 h, whereas for free insulin, the blood glucose levels started to increase 1.5 h post-injection, and returned to baseline after 4 h. Moreover, for INS-GNPs, the blood glucose levels reached 60–70% of baseline values 8.5 hours post-injection (data not shown). The Mann–Whitney *U* test was performed on these results, showing a significant difference between INS-GNPs and free insulin ($p < 0.05$). It is important to note that the injected dose of free insulin used in this study (0.12 IU) is significantly lower than in other studies,[6,11,37–41] which used a range of 0.25–5.00 IU insulin per mouse.

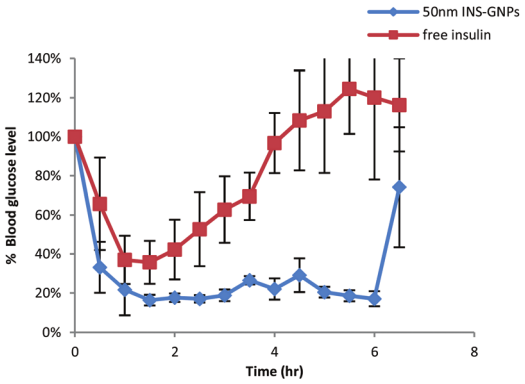

Fig. 7 Effect of INS-GNPs on diabetic mice: 50 nm INS-GNPs (200 μl of 30 mg ml^{-1}) or free insulin (0.12 IU) were intravenously injected into diabetic mice. Blood glucose levels were monitored every 0.5 h, up to 6.5 h post-injection. The results are presented as percentage of blood glucose levels, mean ± S.D. *$p < 0.05$ INS-GNPs *vs.* free insulin. *U*-Test value = 2.82×10^{-11}.

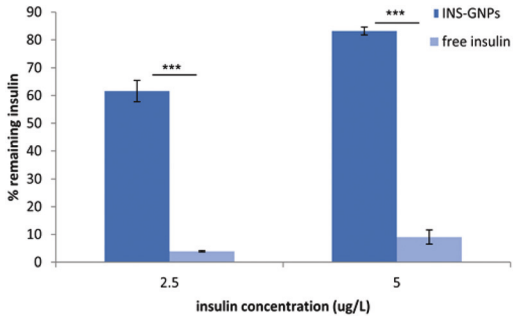

Fig. 8 Comparison between INS-GNPs and free insulin degradation by IDE: INS-GNPs or free insulin, at two identical concentrations, were incubated for 2 h with the insulin-degrading enzyme (IDE). INS-GNPs have significantly higher remaining insulin after IDE digestion, compared to free insulin, which appears to be rapidly degraded. The results are presented as percentage of remaining insulin after IDE digestion, compared to samples without IDE, mean ± S.D. Significant comparisons following Bonferroni correction are marked with asterisks (***$p < 0.001$, **$p < 0.01$, *$p < 0.05$).

Resistance of INS-GNPs to enzymatic degradation. In an attempt to explain the result presented in Fig. 5, showing that an identical amount of insulin has a different effect when connected to a nanoparticle, we examined the long-term resistance of INS-GNPs to degradation. INS-GNPs or free insulin, at two identical concentrations (5, 2.5 μg L^{-1}), were incubated for 2 h with IDE, the major enzyme responsible for insulin degradation.[42–44] The remaining amount of insulin 2 h post-IDE degradation, compared to the same amount without IDE degradation, was measured by ELISA. Two-way ANOVA revealed a significant effect for INS-GNPs ($p < 0.001$), suggesting that free insulin is significantly degraded by IDE, compared to INS-GNPs. *Post-hoc* analysis confirmed that INS-GNPs had significantly larger amounts of insulin remaining following IDE incubation, at all the concentrations tested, compared to free insulin (Fig. 8). These results suggest that the prolonged bioactivity and hypoglycemic effect of the INS-GNP are due to the conjugation of insulin to the GNP, which increases its stability, prevents rapid degradation by IDE and thus allows prolonged bio-activity.

Glucose tolerance test in INS-GNP treated NOD mice. To further investigate the activity of the INS-GNPs *in vivo*, a glucose tolerance test was performed in NOD mice following IV injection of INS-GNPs (30 mg ml^{-1}, 200 μl), or free insulin (0.12 IU) as control. Two hours post initial injection, free glucose was injected (IV) into both groups. In mice that received free insulin, the blood glucose levels gradually returned to baseline after glucose injection (Fig. 9). However, in mice that received INS-GNPs, glucose injection did not significantly affect the blood glucose levels, which remained in the range of 40% of baseline.

The Mann–Whitney *U* test showed a significant difference between INS-GNPs and free insulin ($p < 0.05$). These results indicate that insulin remains active when bound to GNPs for over 5 h post-injection.

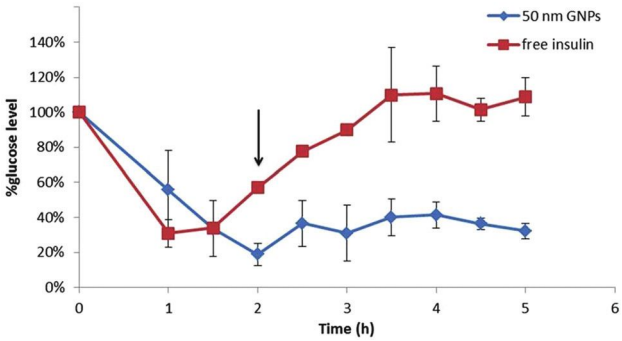

Fig. 9 Glucose tolerance test: 50 nm INS-GNPs (30 mg ml^{-1}, 200 μl) and free insulin (0.12 IU) were intravenously injected into diabetic mice. Free glucose was intravenously injected 2 h post initial injection (black arrow). Blood glucose levels were monitored every 0.5 h, up to 5 h post initial injection. The results are presented as percentage of blood glucose levels, mean ± S.D. *$p < 0.05$ INS-GNPs *vs.* free insulin, *U*-test value = 2.32×10^{-7}.

Bioactivity of subcutaneously injected INS-GNPs into NOD mice. Different routes of insulin administration are needed, and each route affects the duration of insulin activity.[8,11,12,41] To examine another route of insulin administration, 50 nm INS-GNPs (30 mg ml^{-1}, 200 μl), or free insulin (0.12 IU) as control, were subcutaneously injected into NOD mice. As demonstrated in Fig. 10, INS-GNPs showed a prolonged hypoglycemic effect compared to free insulin. The blood glucose levels decreased immediately after the injection of both INS-GNPs and free insulin, and reached their lowest value 2 h post-injection. However, whereas the blood glucose levels of mice treated with free insulin returned to baseline 5 h post-injection, the blood glucose levels of mice treated with INS-GNPs increased to only 50% of baseline 6 h post-injection. The Mann–Whitney *U* test performed on these results showed

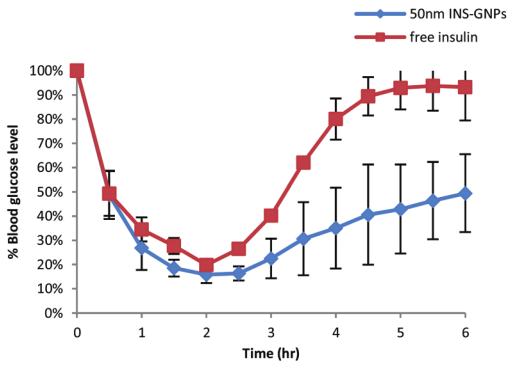

Fig. 10 Profiles of blood glucose levels following subcutaneous administration of free insulin and INS-GNPs in diabetic mice. 50 nm INS-GNPs (30 mg ml^{-1}, 200 μl) or free insulin (0.12 IU) were subcutaneously injected into diabetic mice. Blood glucose levels were monitored every 0.5 h, up to 6 h post-injection. The results are presented as percentage of blood glucose levels, mean ± S.D. *$p < 0.05$ INS-GNPs *vs.* free insulin, *U*-test value = 0.000457.

a significant difference between INS-GNPs and free insulin ($p < 0.05$).

Thus, similar to intravenous injection, these results demonstrate the prolonged bio-activity of subcutaneously injected INS-GNPs, which significantly affects blood glucose levels.

Conclusion

This study demonstrates the adjustable and prolonged effect of INS-GNPs on glucose regulation, which can potentially be used for personalized diabetic treatment. We show, in a mouse model for type 1 diabetes, that our INS-GNPs provide a long-term decrease of blood glucose levels in comparison with free insulin, following both intravenous and subcutaneous injection, and in a glucose tolerance test. The prolonged bio-activity could be explained by the slow degradation of INS-GNPs by IDE compared to free insulin, suggesting that conjugation of insulin to GNPs stabilizes insulin. The results further demonstrate that by controlling the size and concentration of the GNPs one can control the duration of the insulin activity and the minimum glucose level, which potentially can promote personalized treatment for diabetic patients.

Competing financial interests

The authors have declared that no competing interest exists.

Acknowledgements

Funding for this research was provided by Teva Pharmaceutical Industries Ltd as part of the Israeli National Network of Excellence in Neuroscience (NNE) (to MS and RP) and by ISF grant (1092/11) (to DF).

References

1 S. L. Norris, M. M. Engelgau and K. M. Narayan, *Diabetes Care*, 2001, **24**, 561–587.
2 D. M. Nathan, J. B. Buse, M. B. Davidson, E. Ferrannini, R. R. Holman, R. Sherwin and B. Zinman, *Diabetes Care*, 2009, **32**, 193–203.
3 K. D. Barnard, C. E. Lloyd and T. Skinner, *Diabetic medicine: a journal of the British Diabetic Association*, 2007, **24**(6), 607–617.
4 World Health Organisation, can be found under http://www.who.int/mental_health/media/68.pdf, 1999.
5 Z. Gu, A. A. Aimetti, Q. Wang, T. T. Dang, Y. Zhang, O. Veiseh, H. Cheng, R. S. Langer and D. G. Anderson, *ACS Nano*, 2013, **7**, 4194–4201.
6 B. Sarmento, A. Ribeiro, F. Veiga, P. Sampaio, R. Neufeld and D. Ferreira, *Pharm. Res.*, 2007, **24**, 2198–2206.
7 E. M. Pridgen, F. Alexis, T. T. Kuo, E. Levy-Nissenbaum, R. Karnik, R. S. Blumberg, R. Langer and O. C. Farokhzad, *Sci. Transl. Med.*, 2013, **5**, 213ra167.
8 C. Damgé, P. Maincent and N. Ubrich, *J. Controlled Release*, 2007, **117**, 163–170.
9 M. Higaki, M. Kameyama, M. Udagawa, Y. Ueno, Y. Yamaguchi, R. Igarashi, T. Ishihara and Y. Mizushima, *Diabetes Technol. Ther.*, 2006, **8**, 369–374.
10 X. Zhao, Y. Zu, S. Zu, D. Wang, Y. Zhang and B. Zu, *Drug Dev. Ind. Pharm.*, 2010, **36**, 1177–1185.
11 D. R. Bhumkar, H. M. Joshi, M. Sastry and V. B. Pokharkar, *Pharm. Res.*, 2007, **24**, 1415–1426.
12 H. M. Joshi, D. R. Bhumkar, K. Joshi, V. Pokharkar and M. Sastry, *Langmuir*, 2006, **22**, 300–305.
13 K. Nose, D. Pissuwan, M. Goto, Y. Katayama and T. Niidome, *Nanoscale*, 2012, **4**, 3776–3780.
14 Y. Huang, F. Yu, Y.-S. Park, J. Wang, M.-C. Shin, H. S. Chung and V. C. Yang, *Biomaterials*, 2010, **31**, 9086–9091.
15 O. Uchechi, J. D. N. Ogbonna and A. A. Attama, *Application of Nanotechnology in Drug Delivery*, InTech, 2014.
16 I. M. Rodríguez-Cruz, C. L. Domínguez-Delgado, R. Díaz-Torres, A. L. Revilla-Vázquez, N. C. Aléncaster and J. J. Escobar-Chávez, *Recent Advances in Novel Drug Carrier Systems*, InTech, 2012.
17 R. Ankri, H. Duadi, M. Motiei and D. Fixler, *J. Biophotonics*, 2012, **5**, 263–273.
18 R. Ankri, V. Peretz, M. Motiei, R. Popovtzer and D. Fixler, *Int. J. Nanomed.*, 2012, **7**, 449–455.
19 E. E. Connor, J. Mwamuka, A. Gole, C. J. Murphy and M. D. Wyatt, *Small*, 2005, **1**, 325–327.
20 A. I. SHERMAN and M. TER-POGOSSIAN, *Cancer*, 1953, **6**, 1238–1240.
21 T. Reuveni, M. Motiei, Z. Romman, A. Popovtzer and R. Popovtzer, *Int. J. Nanomed.*, 2011, **6**, 2859–2864.
22 R. Arvizo, R. Bhattacharya and P. Mukherjee, *Expert Opin. Drug Delivery*, 2010, **7**, 753–763.
23 P. Ghosh, G. Han, M. De, C. K. Kim and V. M. Rotello, *Adv. Drug Delivery Rev.*, 2008, **60**, 1307–1315.

24 G. Zhang, Z. Yang, W. Lu, R. Zhang, Q. Huang, M. Tian, L. Li, D. Liang and C. Li, *Biomaterials*, 2009, **30**, 1928–1936.
25 C. Lasagna-Reeves, D. Gonzalez-Romero, M. A. Barria, I. Olmedo, A. Clos, V. M. Sadagopa Ramanujam, A. Urayama, L. Vergara, M. J. Kogan and C. Soto, *Biochem. Biophys. Res. Commun.*, 2010, **393**, 649–655.
26 S. K. Balasubramanian, J. Jittiwat, J. Manikandan, C.-N. Ong, L. E. Yu and W.-Y. Ong, *Biomaterials*, 2010, **31**, 2034–2042.
27 J. Lipka, M. Semmler-Behnke, R. A. Sperling, A. Wenk, S. Takenaka, C. Schleh, T. Kissel, W. J. Parak and W. G. Kreyling, *Biomaterials*, 2010, **31**, 6574–6581.
28 N. Chanda, V. Kattumuri, R. Shukla, A. Zambre, K. Katti, A. Upendran, R. R. Kulkarni, P. Kan, G. M. Fent, S. W. Casteel, C. J. Smith, E. Boote, J. D. Robertson, C. Cutler, J. R. Lever, K. V. Katti and R. Kannan, *Proc. Natl. Acad. Sci. U. S. A.*, 2010, **107**, 8760–8765.
29 A. Kunzmann, B. Andersson, T. Thurnherr, H. Krug, A. Scheynius and B. Fadeel, *Biochim. Biophys. Acta*, 2011, **1810**, 361–373.
30 I. H. El-Sayed, *Curr. Oncol. Rep.*, 2010, **12**, 121–128.
31 H. J. Johnston, G. Hutchison, F. M. Christensen, S. Peters, S. Hankin and V. Stone, *Crit. Rev. Toxicol.*, 2010, **40**, 328–346.
32 C. M. Cobley, L. Au, J. Chen and Y. Xia, *Expert Opin. Drug Delivery*, 2010, **7**, 577–587.
33 X.-D. Zhang, H.-Y. Wu, D. Wu, Y.-Y. Wang, J.-H. Chang, Z.-B. Zhai, A.-M. Meng, P.-X. Liu, L.-A. Zhang and F.-Y. Fan, *Int. J. Nanomed.*, 2010, **5**, 771–781.
34 J. Turkevich, P. C. Stevenson and J. Hillier, *Discuss. Faraday Soc.*, 1951, **11**, 55.
35 X. Qian, X.-H. Peng, D. O. Ansari, Q. Yin-Goen, G. Z. Chen, D. M. Shin, L. Yang, A. N. Young, M. D. Wang and S. Nie, *Nat. Biotechnol.*, 2008, **26**, 83–90.
36 G. Sonavane, K. Tomoda and K. Makino, *Colloids Surf., B*, 2008, **66**, 274–280.
37 V. Brezar, S. Culina, M.-C. Gagnerault and R. Mallone, *Eur. J. Immunol.*, 2012, **42**, 1553–1561.
38 D. Bécard, I. Hainault, D. Azzout-Marniche, L. Bertry-Coussot, P. Ferré and F. Foufelle, *Diabetes*, 2001, **50**, 2425–2430.
39 I. Bache, K. H. Jørgensen and K. Buschard, *Diabetes Res. Clin. Pract.*, 1997, **37**, 9–14.
40 Z. Wu, Q. Ping, Y. Wei and J. Lai, *Acta Pharmacol. Sin.*, 2004, **25**, 966–972.
41 Y.-H. Lin, C.-T. Chen, H.-F. Liang, A. R. Kulkarni, P.-W. Lee, C.-H. Chen and H.-W. Sung, *Nanotechnology*, 2007, **18**, 105102.
42 L. Zhao, B. Teter, T. Morihara, G. P. Lim, S. S. Ambegaokar, O. J. Ubeda, S. A. Frautschy and G. M. Cole, *J. Neurosci.*, 2004, **24**, 11120–11126.
43 W. Farris, S. Mansourian, Y. Chang, L. Lindsley, E. A. Eckman, M. P. Frosch, C. B. Eckman, R. E. Tanzi, D. J. Selkoe and S. Guenette, *Proc. Natl. Acad. Sci. U. S. A.*, 2003, **100**, 4162–4167.
44 M. A. Leissring, E. Malito, S. Hedouin, L. Reinstatler, T. Sahara, S. O. Abdul-Hay, S. Choudhry, G. M. Maharvi, A. H. Fauq, M. Huzarska, P. S. May, S. Choi, T. P. Logan, B. E. Turk, L. C. Cantley, M. Manolopoulou, W.-J. Tang, R. L. Stein, G. D. Cuny and D. J. Selkoe, *PLoS One*, 2010, **5**, e10504.

